Original Article

Institution of MECHANICAL ENGINEERS

Journal of ENGINEERING FOR THE MARITIME ENVIRONMENT

Proc IMechE Part M:
J Engineering for the Maritime Environment
226(1) 36–50

DOI: 10.1177/1475090211424002
pim.sagepub.com
SAGE

Performance of a perforated submerged semicircular breakwater due to non-breaking waves

Govindasamy Dhinakaran[1], Vallam Sundar[2], Renganathan Sundaravadivelu[2] and Kai U Graw[3]

Abstract

The present experimental research work focused on how a semicircular breakwater performs hydrodynamically under submerged conditions. In the field, a submerged semicircular breakwater may be preferred in front of the vertical breakwater to mitigate the wave forces and to minimize coastal erosion on its lee side. Various parameters affect the hydrodynamic performance of a semicircular breakwater such as the reflection and transmission characteristics, the dimensionless pressures, the horizontal forces and the vertical forces, and these are considered in the present study. Experiments were performed for three different perforations, namely 7%, 11% and 17%, of the exposed surface area with perforations on its sea side (sea-side perforated) and on both sides (fully perforated) owing to regular and random waves. The effect of the water depth was also studied in addition to the effect of perforation. All the hydrodynamic characteristics considered for the present study on the semicircular caisson are presented as functions of the relative water depth, and optimal conditions were determined. The results on the above-stated variables for sea-side-perforated semicircular breakwaters and fully perforated semicircular breakwaters are compared with the results of an impermeable semicircular breakwater.

Keywords

Submerged breakwaters, perforations, relative water depth, reflection and transmission characteristics, pressure, forces, regular waves, random waves

Date received: 11 May 2011; accepted: 30 August 2011

Introduction

Submerged breakwaters are generally constructed to cause premature breaking of waves so as to protect its shoreward side from the dynamic action of waves. The concept of a semicircular breakwater (SBW) is a recent and newly emerging idea, on which many scientists and researchers all over the world are focusing considerable attention with respect to its hydrodynamic performance. An SBW consists of a semicircularly shaped hollow caisson founded on a rubble mound and cast as different elements and it is made of prestressed concrete. Some of the advantages of an SBW are as follows. The wave force acting on an SBW is less than the force acting on a vertical breakwater, which leads to a lower engineering cost, a smaller overturning moment, no rock fillings inside the caisson, a simpler construction process, a nicer scenery effect, etc. In comparison with aconventional rubble mound breakwater, it has a greater stability against sliding because of its geometry and, hence, it is expected to serve as an offshore-detached breakwater. The type of structure investigated in this study can also be considered as an artificial reef, particularly at locations where the seabed is quite rocky and sediment transport is absent.

Details of the literature on the hydrodynamic performance of a conventional rubble mound submerged breakwater are discussed in the following paragraphs. Ranasinghe and Turner[1] presented instances where submerged breakwaters were both successful and unsuccessful for erosion mitigation, and they found results on

[1]School of Civil Engineering, SASTRA University, India
[2]Department of Ocean Engineering, Indian Institute of Technology Madras, India
[3]Department of Civil Engineering, University of Leipzig, Germany

Corresponding author:
Govindasamy Dhinakaran, School of Civil Engineering, SASTRA University, Thanjavur-613 402, India.
Email: gd@civil.sastra.edu

the shoreline response of such structures. The shoreline response to submerged breakwaters is not fully understood, and therefore Ranasinghe and Turner suggested that the characteristics affecting the shoreline response to submerged structures must be carefully examined.

Ting et al.[2] investigated how the effect of porosity provided in the submerged breakwaters affects non-breaking wave transformations. They selected eight model geometries each with six different porosities, ranging from 0.421 to 0.912, and found that the width of the model has little effect on wave reflection and transmission when the model heights are constant and that the influence of porosity becomes significant as the heights of the models increase.

Some researchers[3–9] also realized the importance of the permeability in near-shore wave transformations and focused on wave-induced flow in a porous structure. Other researchers[10–13] focused on submerged permeable breakwaters for shore protection and carried out numerous theoretical and numerical investigations. Many laboratory and field investigations for this corresponding issue have also been carried out by many researchers.[14–18]

Cokgor and Sedat Kapdasli[19] studied wave transmission in slightly submerged breakwaters with respect to the porosity and the crest height-to-water depth ratio. The similarity between a long shore bar and a dynamic stable submerged breakwater was also studied in one set of the experiments and it was found that both perform in a similar way. Sidek et al.[20] conducted a series of tests to study the effect of the porosity of submerged breakwater model structures with three different porosities ranging from 0.40 to 0.80 and found that transmission increased with increasing model porosity. Jeng et al.[21] studied the interaction between water waves, a submerged breakwater, a vertical wall and a sandy seabed as a laboratory experiment and concluded that the wave-induced pore pressure beneath the submerged breakwater was greater than that at the toe. Chen et al.[22] performed experiments on wave transformation between a submerged permeable breakwater and a seawall including variations in the wave profile, the piling-up of water and the wave run-up and found that the wave height transformation behind the submerged breakwater varies spatially owing to the transmitted wave reflected from the seawall.

Aburatani et al.[23] reported field tests on an SBW built at the Port of Miyazaki, Japan and reported that the wave pressure data confirmed a reduction in the horizontal force component due to the occurrence of a phase difference in the wave pressure on the circumference. In addition, it was stated that the sliding resistance increases because of the simultaneous horizontal wave force component and vertical downward force component. Xie[24,25] has given a new calculation method to estimate the wave forces acting on a submerged SBW and its design, verified with the results of seven related physical model tests, and adopted in the design of a southern estuary jetty of the Yangstze River estuary of the People's Republic of China.

Recently, the present authors[26–28] carried out extensive experimental research on impermeable and sea-side-perforated SBWs and published their results on the hydrodynamic performance under surface piercing conditions to understand the effects of perforations, water depth and rubble mound height. Since then, there has been very little literature published on submerged SBWs; the present work was instigated in order to understand the effects of perforations and the water depth on the hydrodynamic characteristics of submerged sea-side perforated SBWs and fully perforated SBWs.

Experimental investigations

Test facility

The present experimental study was carried out in the Department of Ocean Engineering, Indian Institute of Technology Madras, India, in a wave flume of 72.5 m × 2.0 m × 2.7 m size which is capable of generating both regular and random waves. The water depth in this flume varied from 0.4 m to 2 m. One personal computer was connected to a servo actuator and used to give the input values such as the wave height and the wave period to the wave maker; the same set-up was used for data acquisition on the signals from wave probes and pressure transducers through an amplifier. A six-component force balance was available at a distance of 46 m from the wave maker and it is a permanent facility in the wave flume to measure forces on the breakwater model. Since the breakwater model was mounted on the force balance, the gap between the wave generator and the breakwater was chosen to be 46 m. The waves were generated in such a way that breakwater models were subjected to a sufficient number of waves depending upon the wave periods and also ensured that the wave maker was not subjected to re-reflected waves. The wave maker was inclined accordingly. The details of the flume together with the positions of the wave gauges and the model are shown in Figure 1.

Test model set-up

The model consists of two parts: the bottom frame and the top semicircularly shaped caisson. The caisson was made with aluminium sheet 1 mm thick rolled into a semicircular shape of radius 0.5 m. This sheet fixed to a bottom frame of 50 mm height made from Indian Standard Angle material (50 mm × 50 mm). Rods of 12 mm diameter as stiffeners were provided at the ends and at the centre of the hollow semicircular caisson in order to provide the necessary rigidity for the wall of the model. A flat with dimensions 30 mm × 3 mm was provided along the inner surface of the semicircular caisson to retain the shape. The caisson was fabricated in two units to facilitate easier handling. The central part of the caisson of about 200 mm width was fabricated using Perspex sheet 4 mm thick, onto which the pressure transducers were fixed with uniform spacing

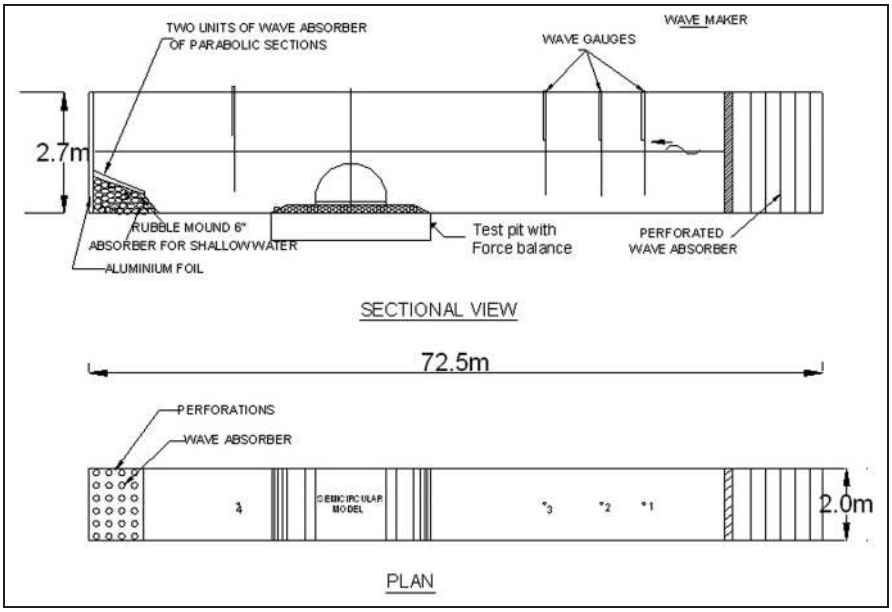

Figure 1. Experimental set-up for the study.

to measure the hydrodynamic pressure at various locations of the model. The bottom frame was fabricated using Indian Standard Medium Channel material (100 mm × 50 mm). It was ensured that this frame did not contact the flume sidewalls or the flume floor. The scale adopted for the study was 1:20 and was derived from the rear dissipating SBW available in the Port of Miyazaki, Japan. The mound was formed using coarse aggregates (granite stones) of weight varying from 50 gf to 100 gf. The slope of 1:2 was maintained on both sides. Two frames of width 25 mm and height 120 mm were initially fabricated and kept on either side of the caisson. A gap of 5 mm was maintained between the caisson and the frames on either side. By providing a 5 mm gap between the frame in which the rubble mound was placed and the caisson, it was ensured that the force exerted on the caisson was measured only by the six-component force balance. The rubble mound was placed on this frame; thus its height h_r was maintained at 120 mm. Hence, for this model its total height h_t is equal to h_r plus the height h_s of the caisson plus the height of the bottom frame (which equals 50 mm), i.e. (0.12 + 0.5 + 0.050) m = 0.67 m. The percentage of perforations in the present work was calculated with reference to the total exposed area of the model to the waves. For example, in the case of sea-side-perforated SBW, the quadrant face of SBW on the sea side was taken as the exposed area from which perforations of 7%, 11% and 17% were chosen by choosing the size of perforations as 15 mm, 20 mm and 25 mm respectively and the shape of perforation as a circle. The centre-to-centre distance between the perforations was taken as a constant value of 50 mm to limit the number of experiments. Similarly, for the fully perforated SBW, the total area of the semicircular caisson was taken as the reference since both the quadrants will be effective dissipating energy in transmission. In all the cases the perforations were distributed uniformly with a centre-to-centre spacing of 50 mm in a grid form. Details of model and instrumentation have already been made available in the earlier publications of the present authors[28,29] and hence are not included in this paper.

Instrumentation used

In order to obtain the incident and reflected wave heights from the structure, three wave gauges were positioned in front of the structure 7 m away from the breakwater model. The distances between the gauges, which were a function of the wave period, were calculated by considering the requirements, and the positions of the wave gauges were changed accordingly. One wave probe was kept on the leeward direction of the model to register the transmitted wave height. The SBW model was subjected to the action of regular and random waves, of periods ranging from 0.8 s to 2 s at intervals of 0.2 s. For each wave period, five different wave heights ranging from 0.03 m to 0.18 m at intervals of 0.03 m were generated. Thus, one test set-p of the model was subjected to about 35 combinations for regular and random waves respectively. The experiments were performed with the model mounted on the six-component force balance. The force balance (R67) measures six components in a rectangular coordinate system. The resolution of the resulting force to be measured into the six components was realized mechanically by way of spring joints, and measurement of the individual components was unaffected with the help of strain-gauge-type force transducers.

All parts of the force balance are made of hard steel with good corrosion resistance against water. The six transducers were waterproofed and can be used to a

depth of 5 m. The balance was mounted in a recess at the bottom of the flume floor and has a platform of (850 mm × 850 mm) flush with the flume floor. The platform was suspended with six coupling rods with flexures at the both the ends and six force transducers. The force transducers were connected to a frame. In the direction of wave propagation, one force component X was measured. Vertically, the three components Z_1, Z_2 and Z_3 were measured at distances 900 mm apart. The side of the force balance with the Z_3 transducer was placed towards the wave maker. The force transducers were connected to a data acquisition system through carrier frequency amplifiers. The sensitivity of the transducers at their rated loads is about ± 2 mV/V, which means that, even for much smaller forces than the rated loads, the amplifiers can give a full-scale indication. The force balance initially was calibrated before starting the experiments and again after completing the experiments. Both the calibration values were the same. The calibration of force balance was performed by placing known weights and recording the corresponding voltages. A spring balance was used to measure the horizontal pull and the corresponding voltage was noted. The model was fixed to the force balance consisting of a machined stainless steel plate of about 12 mm thickness with 36 threaded borings using M_{12} stainless steel bolts.

Results and discussion

General comments

Reflection analysis was carried out using the fixed three-wave probe method and the distance between the wave gauges was a function of the wave period. The wave analysis software Wave Synthesizer 4 installed together with the wave maker supplied by Danish Hydraulic Institute was used for the analysis. The wave reflection analysis was used in connection with model tests in a flume to calculate the spectrum of progressive waves, the reflection function and the average reflection coefficient. The basic method for the frequency domain separation of the wave time series into a time series of progressive and reflected waves was extended to include concurrent recordings from several wave gauges. The governing equations were solved using a least-squares fitting approach. The input data for the analysis are the surface elevation time series from the wave gauges, the wave gauge position given along a coordinate axis with a positive orientation in the wave propagation direction, the water depth in the wave flume and the number of degrees of freedom to be used in the spectral smoothening. For irregular waves, the peak wave period and the significant wave height H_s were used, and the Pierson–Moskowitz spectrum was utilized as representative.

The experimental results from the fully perforated SBW models (perforations provided on both sides of the breakwater) were compared with the impermeable SBW (no perforation on either side of the breakwater) and sea-side-perforated SBW models (perforation provided on the seaward side) reported by Dhinakaran et al.[29] to study the effect of perforation and the influence of the water depth.

Reflection characteristics

The variations in the reflection coefficient with the relative water depth for the SBW0, SBW7, SBW11, SBW17, SBWf7, SBWf11 and SBWf17 models for h_w/h_t = 1.0, 1.2 and 1.4 for a constant h_r/h_t = 0.18 due to regular waves are presented in Figure 2 to understand the effects of both the perforations and the water depth. The value of the reflection coefficient varies from 0.18 to 0.38 for SBW0, whereas these values are from 0.16 to 0.35, from 0.13 to 0.31, from 0.15 to 0.32, from 0.11 to 0.27, from 0.09 to 0.20 and from 0.08 to 0.18 for SBW7, SBW11, SBW17, SBWf7, SBWf11 and SBWf17 respectively. The results indicate that the reflection coefficient decreases with an increase in h_w/L for all the h_w/h_t values tested and for all the models of the impermeable, the sea-side-perforated and the fully perforated SBWs tested. This is because, when waves of shorter length run over the submerged model, the presence of the model does not influence the energy dissipation process of waves and hence there is less reflection for higher h_w/L values. For waves of long period, the energy dissipated was greater and hence there was more reflection. The reflection coefficient decreases with an increase in perforation up to 11% and it increases with a further increase in perforations to 17% for sea-side-perforated SBW, which indicates the limitation of the percentage of perforations to be provided in a model. For fully perforated SBWs, an increase in the percentage of perforations results in a decrease in reflection, since more waves are transmitted owing to the increase in the percentage of perforations.

The variations in the average reflection coefficients with the relative water depth for the SBW0, SBW7, SBW11, SBW17, SBWf7, SBWf11 and SBWf17 models for h_w/h_t = 1.0, 1.2 and 1.4 for a constant h_r/h_t = 0.18 due to random waves are reported in Figure 3. The value of the reflection coefficient varies from 0.21 to 0.35 for SBW0, whereas these values are from 0.17 to 0.27, from 0.15 to 0.23, from 0.17 to 0.25, from 0.12 to 0.20, from 0.11 to 0.19 and from 0.09 to 0.13 for SBW7, SBW11, SBW17, SBWf7, SBWf11 and SBWf17 respectively. In the case of random waves, for a lower relative water depth, the reflection coefficients were slightly higher and higher energy dissipation occurs owing to uneven wave heights. Here also SBW17 shows the reverse trend. Considering the effect of the water depth, for regular waves, the reflection coefficient decreases with increase in h_w/h_t. This is the reason why, when h_w/h_t increases, the influence of waves on the SBW model is reduced, resulting in less reflection. In the case of random waves, an increase in h_w/h_t from 1.0 to 1.2 increases the reflection coefficient and a further increase in h_w/h_t to 1.4 decreases the reflection coefficient. This occurs because of random waves of various

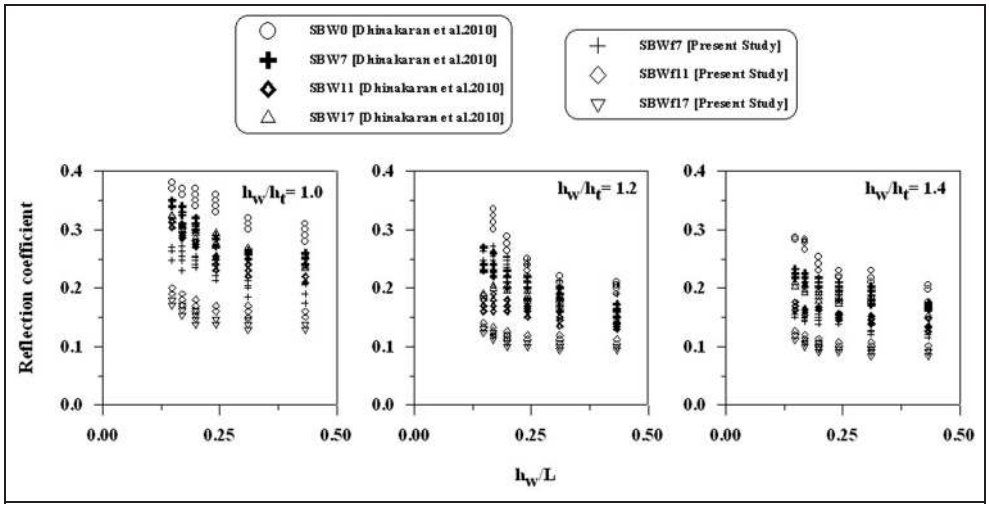

Figure 2. Effect of perforations on the reflection coefficient due to regular waves.

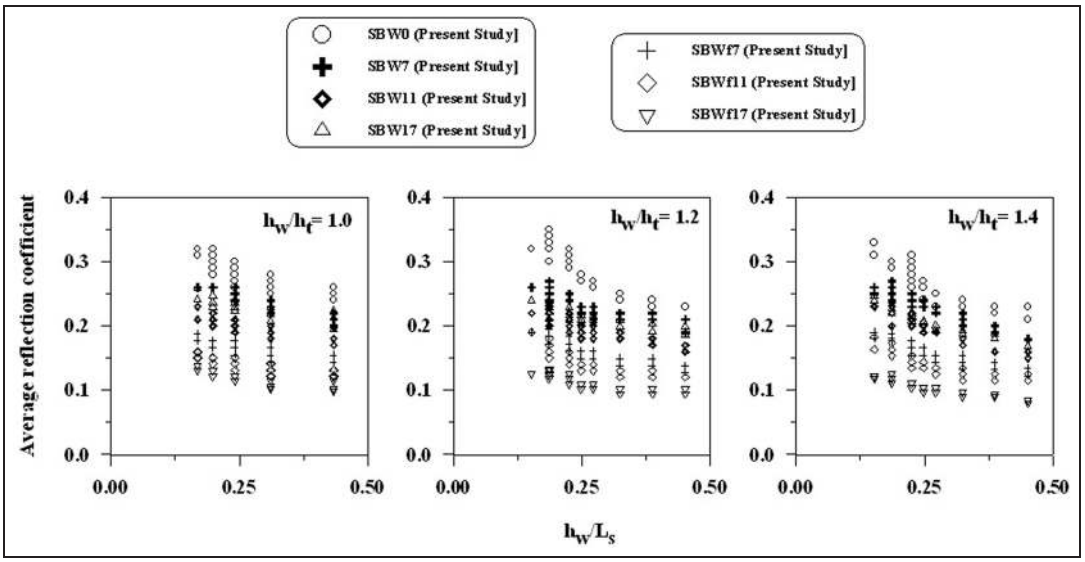

Figure 3. Effect of perforations on the average reflection coefficient due to random waves.

wave height and, for $h_w/h_t = 1.2$, the SBW model feels the effect of waves. Since for $h_w/h_t = 1.4$ the difference in elevation was 0.27 m, the influence of waves was insignificant in the SBW model and hence there is more transmission, resulting in less reflection and lower loss.

Transmission characteristics

The variations in the transmission coefficient with the relative water depth for the SBW0, SBW7, SBW11, SBW17, SBWf7, SBWf11 and SBWf17 models for $h_w/h_t = 1.0$, 1.2 and 1.4 for a constant $h_r/h_t = 0.18$ due to regular waves are reported in Figure 4. The variation in the transmission coefficient decreases with increase in the relative water depth perforations from 7% to 17% in the case of sea-side-perforated SBW for $h_w/h_t = 1.0$ and was found to be less than for the impermeable SBW. This was because energy dissipation was much less owing to the curvature and hence smooth transmission of waves was observed for an impermeable SBW. It should be noted that, for $h_w/h_t = 1.0$, the crest of the SBW model and the water depth were the same. In the case of the sea-side-perforated SBW, the provision of perforations creates turbulence, resulting in energy dissipation, and affects the transmission of waves. For a fully perforated SBW, the transmission increases with increasing percentage of perforations. In the case of the SBW model with $h_w/h_t = 1.2$ and 1.4, the transmission increases with increasing percentage of perforations and, especially for $h_w/h_t = 1.4$, the effect of the perforations was insignificant. The variation in the transmission coefficient increases with increase in the relative water depth; this arose because more dissipation was observed with long waves and less dissipation for shorter waves. The transmission coefficient for $h_w/h_t = 1.0$ varies from 0.31 to 0.61, from 0.38 to 0.72 and from 0.43 to 0.83 for SBWf7, SBWf11 and SBWf17

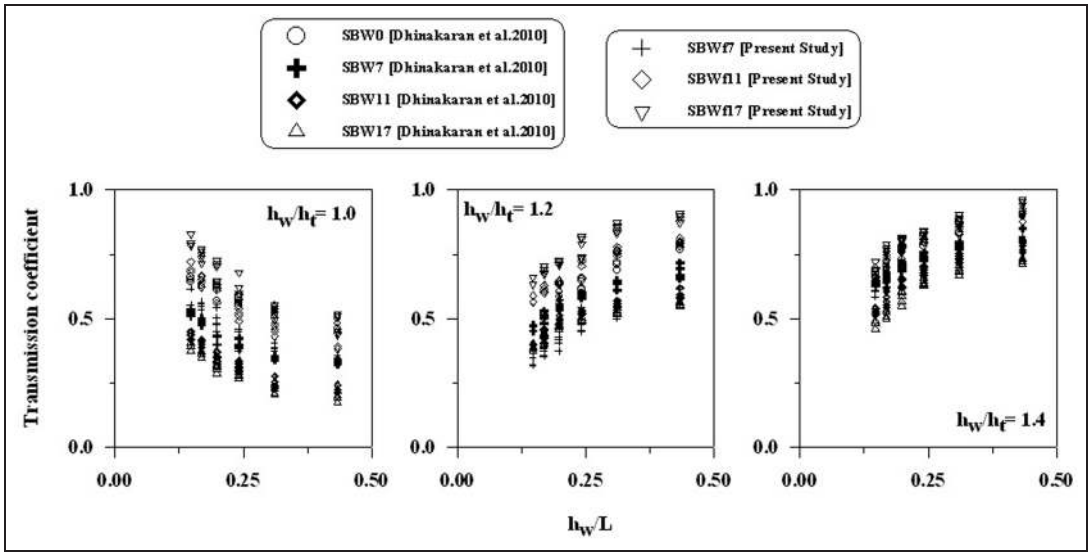

Figure 4. Effect of perforations on the transmission coefficient due to regular waves.

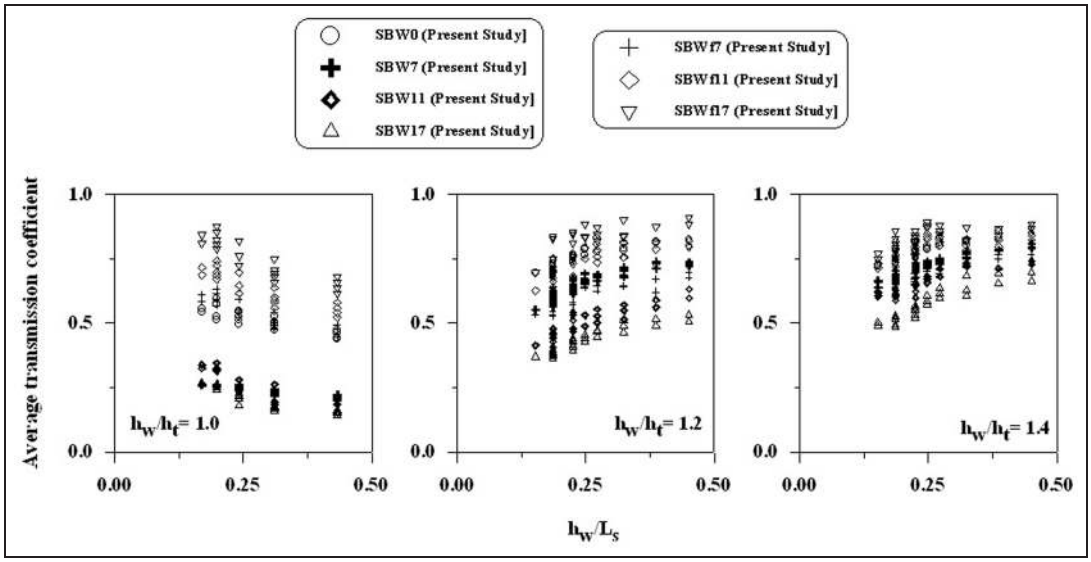

Figure 5. Effect of perforations on the average transmission coefficient due to random waves.

respectively. These values were from 0.31 to 0.61, from 0.56 to 0.81 and from 0.63 to 0.90 respectively for h_w/h_t = 1.2 and from 0.58 to 0.82, from 0.65 to 0.92 and from 0.68 to 0.96 respectively for h_w/h_t = 1.4. The variations in the average transmission coefficient with relative water depth for SBW0, SBW7, SBW11, SBW17, SBWf7, SBWf11 and SBWf17 models for h_w/h_t = 1.0, 1.2 and 1.4 for a constant h_r/h_t = 0.18 due to random waves are reported in Figure 5. A similar trend was also observed in random waves, but energy dissipation was slightly more owing to the various wave heights, resulting in lower transmission compared with regular waves. The average transmission coefficient due to random waves for h_w/h_t = 1.0 varies from 0.44 to 0.61, from 0.52 to 0.72 and from 0.61 to 0.84 for SBWf7, SBWf11 and SBWf17 respectively. These values were from 0.53 to 0.69, from 0.62 to 0.82 and from 0.69 to 0.90 respectively for h_w/h_t = 1.2 and from 0.60 to 0.78, from 0.71 to 0.84 and from 0.75 to 0.88 respectively for h_w/h_t = 1.4.

Energy loss

The loss coefficient was calculated from the formula $K_l = \sqrt{1 - \left(K_r^2 + K_t^2\right)}$. The variations in the loss coefficient with the relative water depth for SBW0, SBW7, SBW11, SBW17, SBWf7, SBWf11 and SBWf17 models for h_w/h_t = 1.0, 1.2 and 1.4 for a constant h_r/h_t = 0.18 due to regular waves are reported in Figure 6. The loss coefficient increases with increase in the relative water depth for h_w/h_t = 1.0 and shows the reverse trend for the other two cases of h_w/h_t = 1.2 and 1.4 both for regular waves and for random waves. The loss coefficient due to regular waves for h_w/h_t = 1.0 varies from 0.33 to 0.63, from 0.25 to 0.59 and from 0.15 to 0.54 for

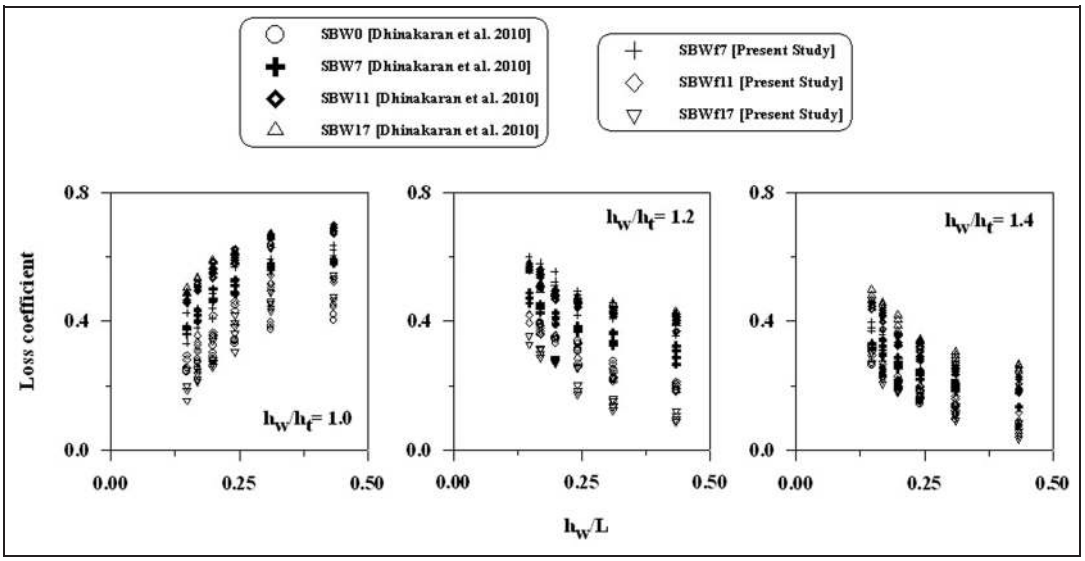

Figure 6. Effect of perforations on the loss coefficient due to regular waves.

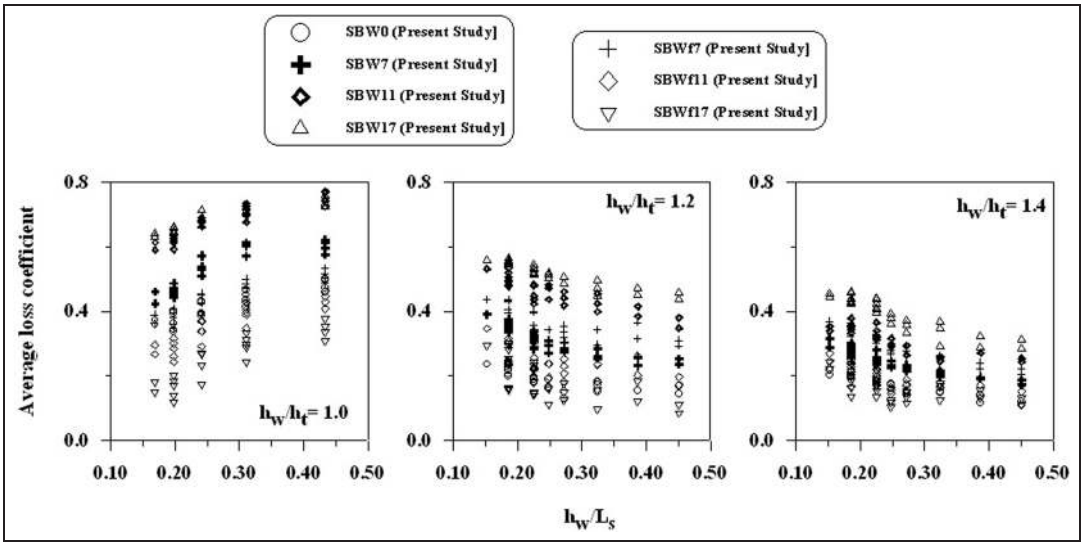

Figure 7. Effect of perforations on the average loss coefficient due to random waves.

SBWf7, SBWf11 and SBWf17 respectively. These values were from 0.35 to 0.60, from 0.18 to 0.42 and from 0.10 to 0.35 respectively for $h_w/h_t = 1.2$ and from 0.17 to 0.39, from 0.06 to 0.32 and from 0.04 to 0.30 respectively for $h_w/h_t = 1.4$. The variations in the average loss coefficient with the relative water depth for SBW0, SBW7, SBW11, SBWf7, SBWf11 and SBWf17 models for $h_w/h_t = 1.0$, 1.2 and 1.4 for a constant $h_r/h_t = 0.18$ due to random waves are presented in Figure 7. The average loss coefficient due to random waves for $h_w/h_t = 1.0$ varies from 0.40 to 0.53, from 0.29 to 0.46 and from 0.17 to 0.37 for SBWf7, SBWf11 and SBWf17 respectively. These values were from 0.29 to 0.43, from 0.17 to 0.34 and from 0.08 to 0.29 respectively for $h_w/h_t = 1.2$ and from 0.20 to 0.37, from 0.15 to 0.26 and from 0.11 to 0.29 respectively for $h_w/h_t = 1.4$. From the results, it was observed that a maximum of 63% of wave energy was lost for $h_w/h_t = 1.0$ and a maximum of 60% of wave energy was lost for $h_w/h_t = 1.2$. Hence, the submerged SBW appeared to be beneficial when utilized in front of the vertical breakwater to minimize the force acting on it, and the dimensions of the vertical breakwater can be reduced accordingly.

Dynamic pressures on the SBW

The variations in the dimensionless shoreward pressure with respect to the relative water depth for SBW0, SBW7, SBW11, SBW17, SBWf7, SBWf11 and SBWf17 models for $h_w/h_t = 1.0$, 1.2 and 1.4 for a constant $h_r/h_t = 0.18$ due to regular waves are depicted in Figures 8, 9 and 10 respectively to understand the effects of perforations and the water depth. The variations in the dimensionless pressure are shown in Figure 8 for three

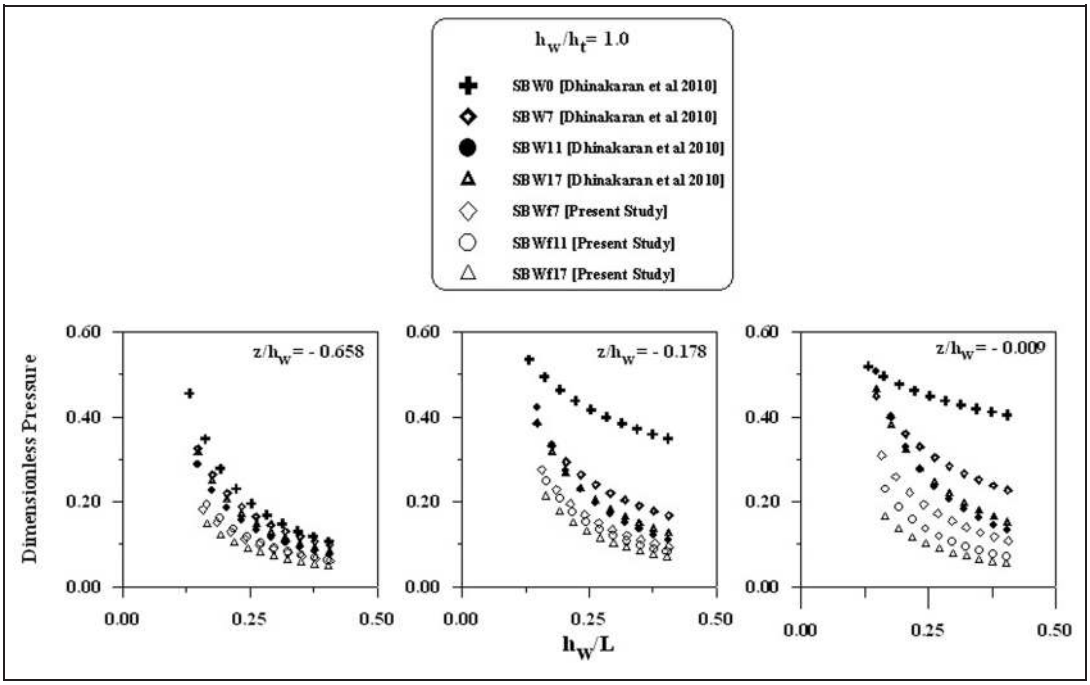

Figure 8. Effect of perforations on the dimensionless pressure due to regular waves for h_w/h_t = 1.0.

different pressure port locations: one at the top position (z/h_w = –0.009), the second at the middle position (z/h_w = –0.178) and the third at the bottom position (z/h_w = –0.658) of the model for h_w/h_t = 1.0. At the bottom location of the model, the pressure decreases with increase in the percentage of perforations both in the sea-side-perforated SBWs and the fully perforated SBWs except that SBW17 in the sea-side-perforated SBWs and SBWf11 in the fully perforated SBWs show the reverse trend. The maximum magnitudes of the dynamic pressure were observed to be 0.43 times, 0.32 times and 0.19 times the static pressure for the impermeable SBWs, the sea-side-perforated SBWs and the fully perforated SBWs respectively. For other pressure port locations, the maximum dynamic pressure of SBW11 is more than those of the other models in that category. However, in the case of the fully perforated SBW models the pressure decreases with increase in the percentage of perforations. At the middle position of the pressure port, the maximum magnitudes of dynamic pressure were observed to be 0.58 times, 0.44 times and 0.28 times the static pressure, and at the top position (near surface of the model) these values were 0.53 times, 0.52 times and 0.35 times the static pressure for the impermeable SBWs, the sea-side-perforated SBWs and the fully perforated SBWs respectively. The results also indicate that the increase in the water depth decreases the pressure except for the pressure port location near the water surface. In the location near to the water surface, an intermittence effect occurs. Figure 9 depicts the variations in the dimensionless pressure for various SBWs. Since the top surface of the model was submerged into water to a depth of 0.13 m, the influence of the percentage of perforations on the variation in the dimensionless pressure was insignificant at the bottom pressure port location. However, the variations observed at the other pressure port locations are significant, especially at the top pressure port. The maximum dynamic pressures for the bottom pressure port were observed to be 0.37 times, 0.31 times and 0.15 times the static pressure, for the middle pressure port the values were 0.52 times, 0.39 times and 0.25 times the static pressure and, for the top pressure port, the values were 0.73 times, 0.53 times and 0.29 times the static pressure for the impermeable SBWs, the sea-side-perforated SBWs and the fully perforated SBWs respectively. Similar observations were noted for h_w/h_t = 1.4, where the top surface of the model was submerged in water to a depth of 0.27 m and hence the effects of the water depth and perforations were less pronounced.

Figures 11 to 13 show the results of the variations in the dimensionless water pressure for random waves for different h_w/h_t values and different pressure port locations in order to understand the effect of the water depth. The maximum dynamic pressure was observed to be higher than for the regular waves and these values for an impermeable SBW were 1.04, 1.95 and 1.35 times the static pressure in the bottom, middle and top locations of the pressure port respectively for h_w/h_t = 1.0. These values for sea-side-perforated SBWs were 0.85, 1.38 and 0.89 times the static pressure and for fully perforated SBWs were 0.49, 0.88 and 0.64 times the static pressure respectively. In the case when h_w/h_t = 1.2, the dimensionless pressure increases from bottom to top pressure port locations. Figures 14 and 15 depict the variations in the dimensionless pressure for regular and random waves for more or less similar pressure port locations at different h_w/h_t values in

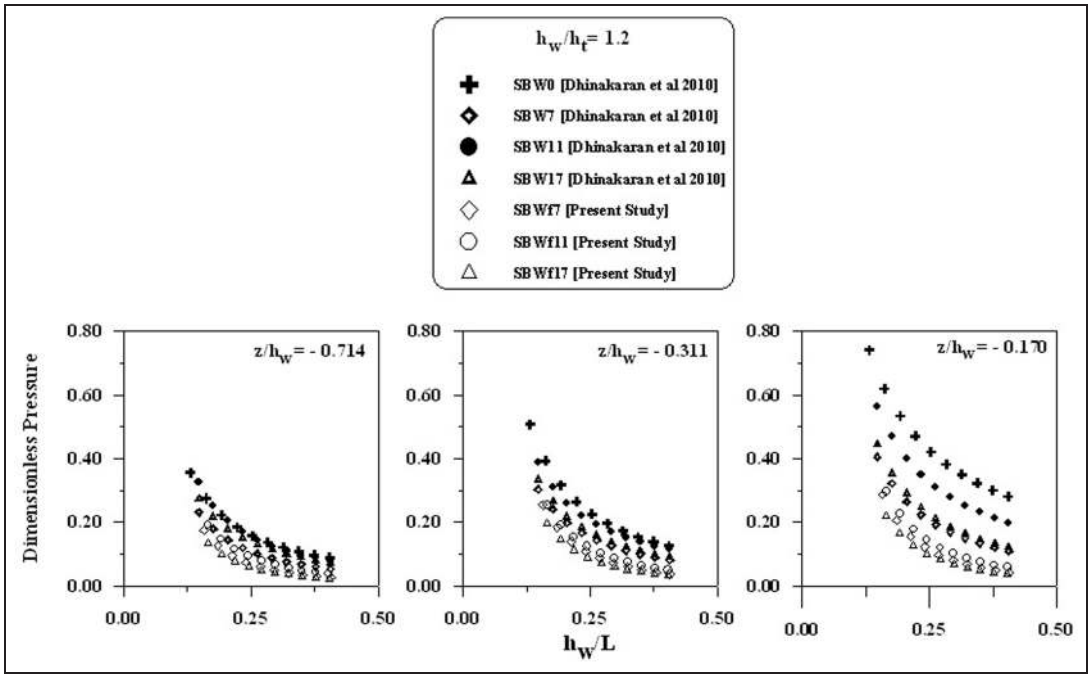

Figure 9. Effect of perforations on the dimensionless pressure due to regular waves for h_w/h_t = 1.2.

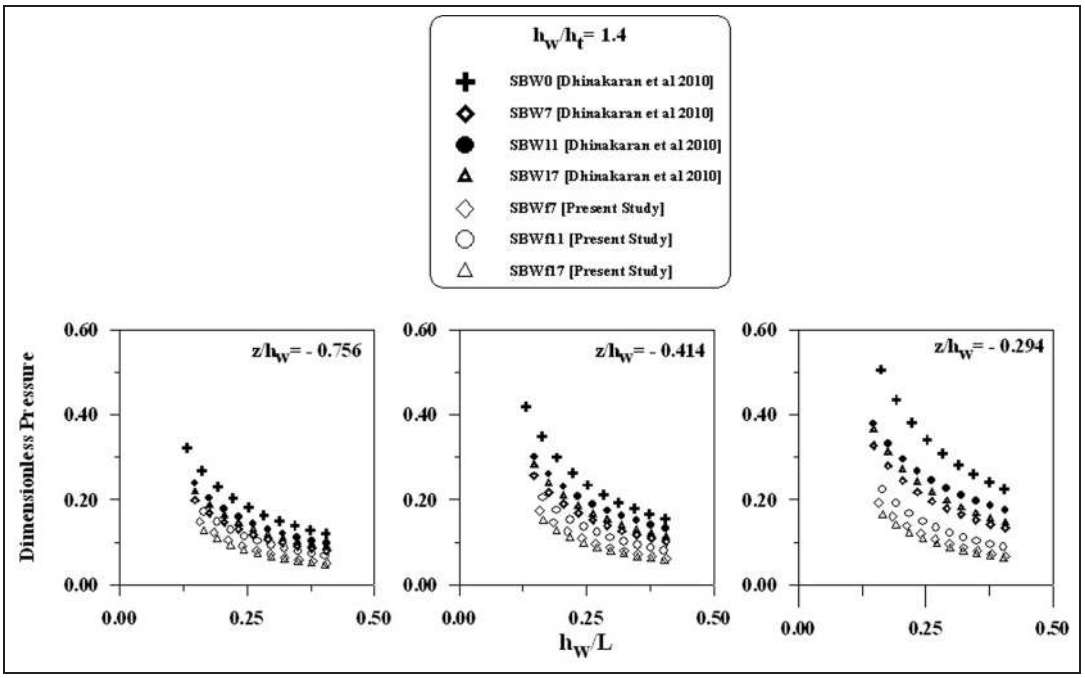

Figure 10. Effect of perforations on the dimensionless pressure due to regular waves for h_w/h_t = 1.4.

order to understand the effect of perforation on the water depth. The effect of the water depth was insignificant and a small variation was found between the results for $h_w/h_t = 1$ and those for $h_w/h_t = 1.2$. However, a lower pressure was observed for $h_w/h_t = 1.4$ irrespective of the percentage of perforations and type (whether the sea-side-perforated or the fully perforated cases), since the SBW model was 0.27 m below the free water surface. Hence, the model was subjected to lower pressure. The present authors have also compared the other port locations in order to understand the effect of perforations on the water depth and found that a similar trend was observed. Only one such comparison is discussed in this paper for the benefit of potential readers so that this effect can be understood.

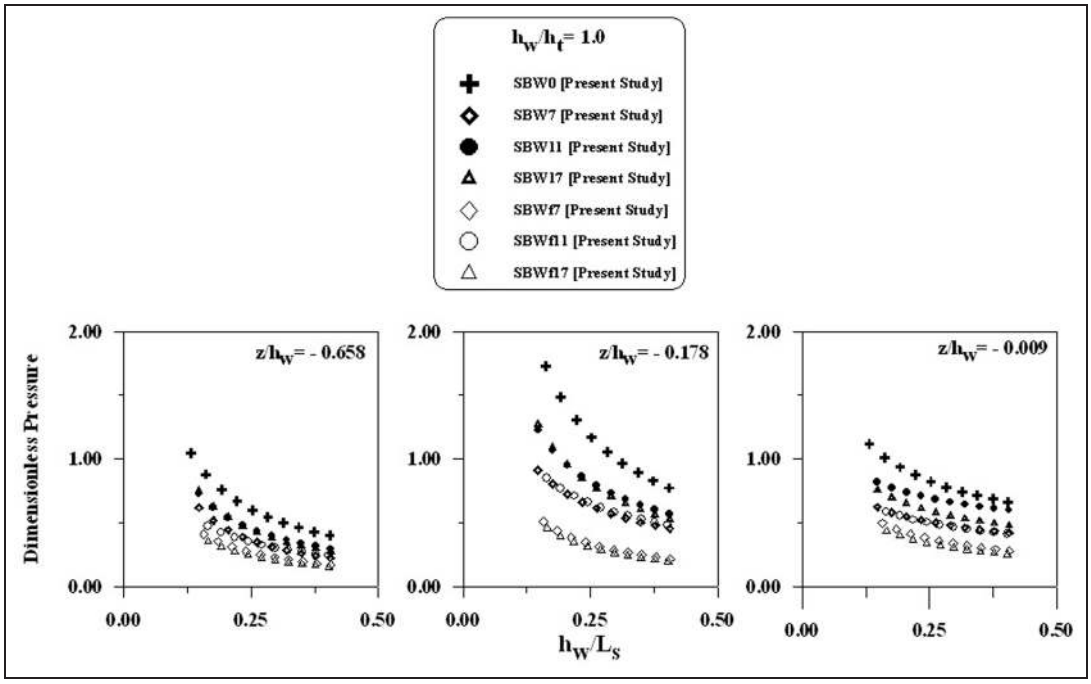

Figure 11. Effect of perforations on the dimensionless pressure due to random waves for h_w/h_t = 1.0.

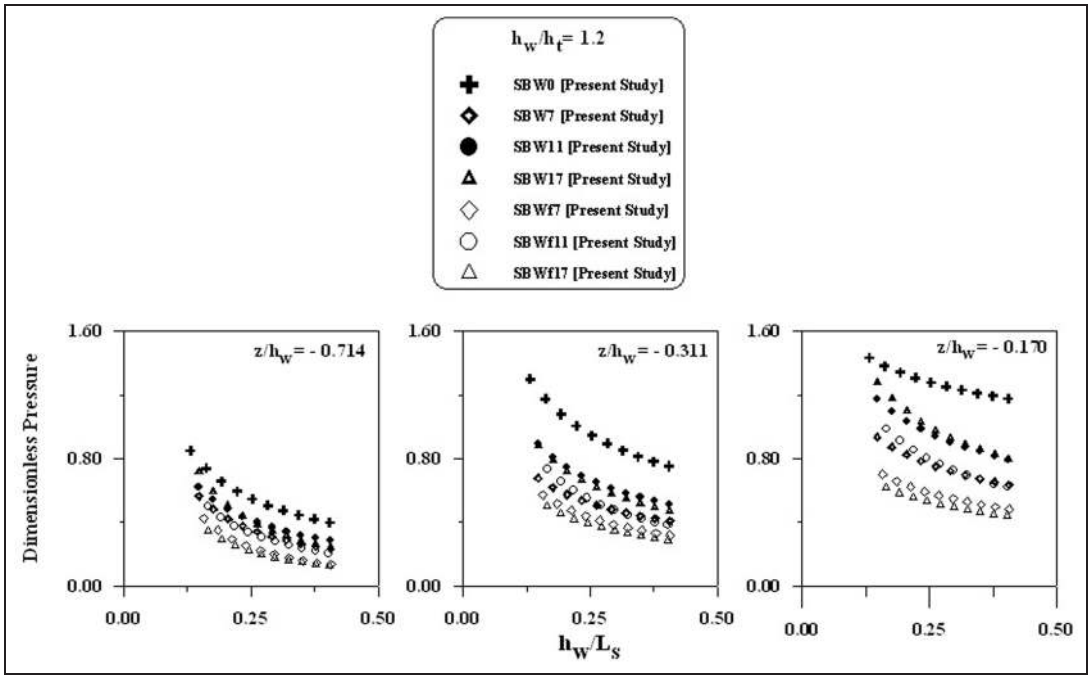

Figure 12. Effect of perforations on the dimensionless pressure due to random waves for h_w/h_t = 1.2.

Forces on the semicircular caisson

The shoreward horizontal force and the vertical force exerted on the semicircular caisson in the presence of the submerged mound measured were normalized by dividing them by γalH. The variations in the dimensionless shoreward horizontal force and the dimensionless vertical force on SBW0, SBW7, SBW11, SBW17, SBWf7, SBWf11 and SBWf17 for three different h_w/h_t ratios are shown in Figures 16 and 17 for regular waves and in Figures 18 and 19 for random waves. The horizontal force component was found to decrease with increase in h_w/L irrespective of the type of SBW. This is because long-period waves exert more force on the caisson and short-period waves transfer less force. An increase in the size of the perforations resulted in the dissipation of more energy in the case of the fully perforated SBW and hence the force decreased

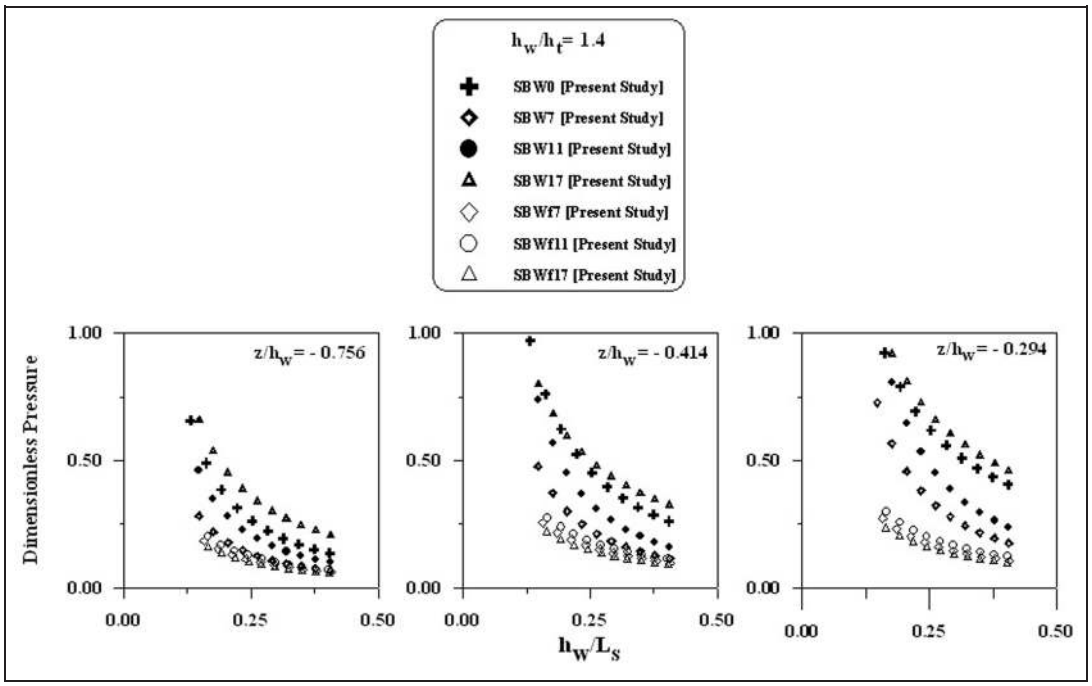

Figure 13. Effect of perforations on the dimensionless pressure due to random waves for $h_w/h_t = 1.4$.

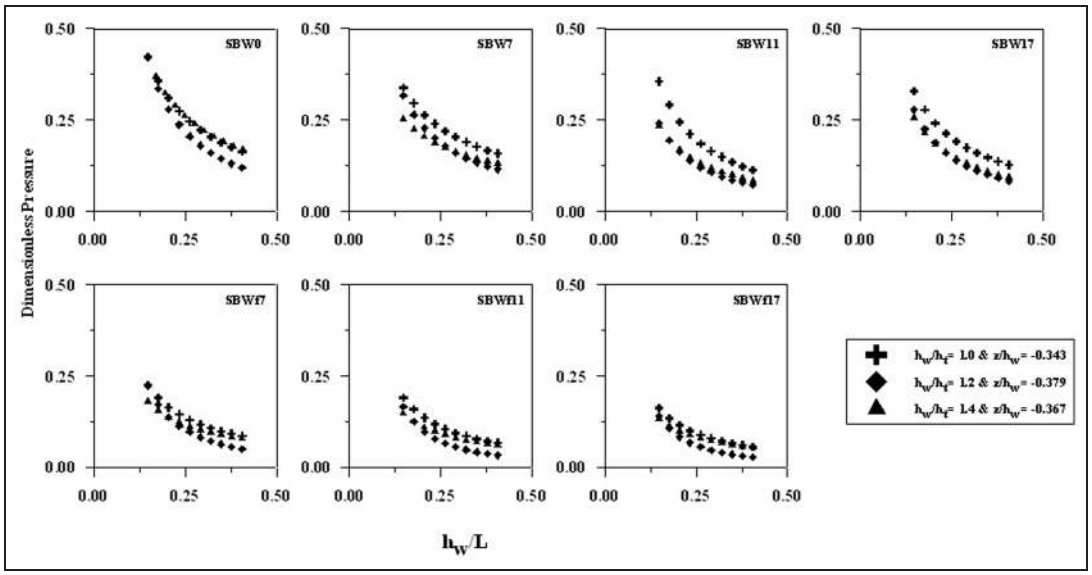

Figure 14. Effect of the water depth on the dimensionless pressure due to regular waves.

accordingly. This is applicable to both the horizontal force and the vertical force. The increase in h_w/h_t increases the forces on the semicircular caisson from $h_w/h_t = 1.0$ to $h_w/h_t = 1.2$ and a further increase to $h_w/h_t = 1.4$ decreases the forces on the caisson. The energy dissipation was observed to be greater for $h_w/h_t = 1.0$ and in this case the water depth and the height of the model were the same. Moderate energy dissipation was observed for $h_w/h_t = 1.2$. Similar trends were observed for both the horizontal force and the vertical force and for both regular waves and random waves. The magnitude of the dimensionless horizontal force was found to be much less than the dimensionless vertical force experienced by the model. The magnitude of the maximum dimensionless vertical force was almost four times the dimensionless horizontal force for both regular waves and random waves and for all h_w/h_t tested.

Conclusions

Detailed experimental investigations were carried out to study the wave transformation characteristics on fully perforated SBW models with 7%, 11%, and 17%

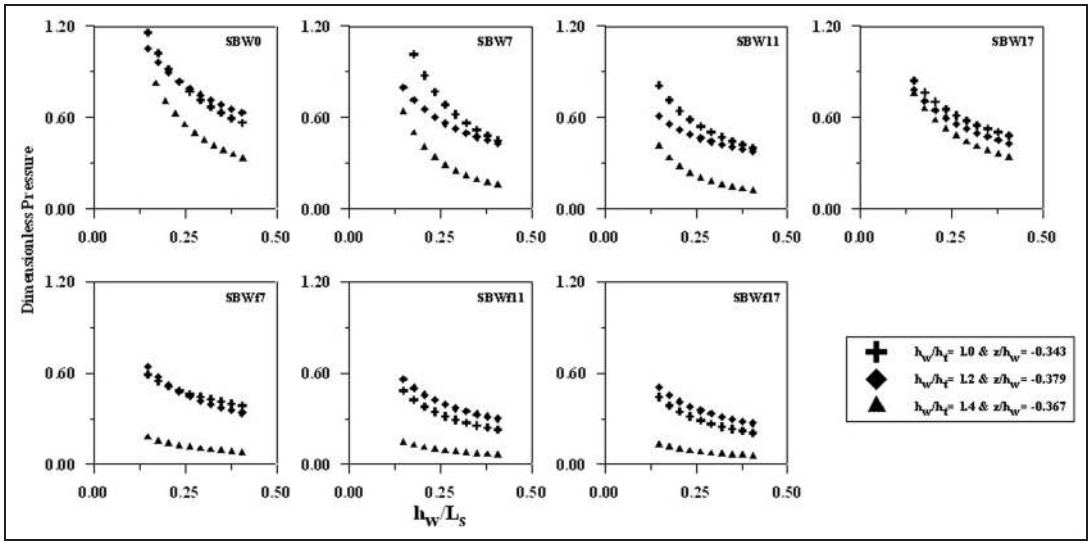

Figure 15. Effect of the water depth on the dimensionless pressure due to random waves.

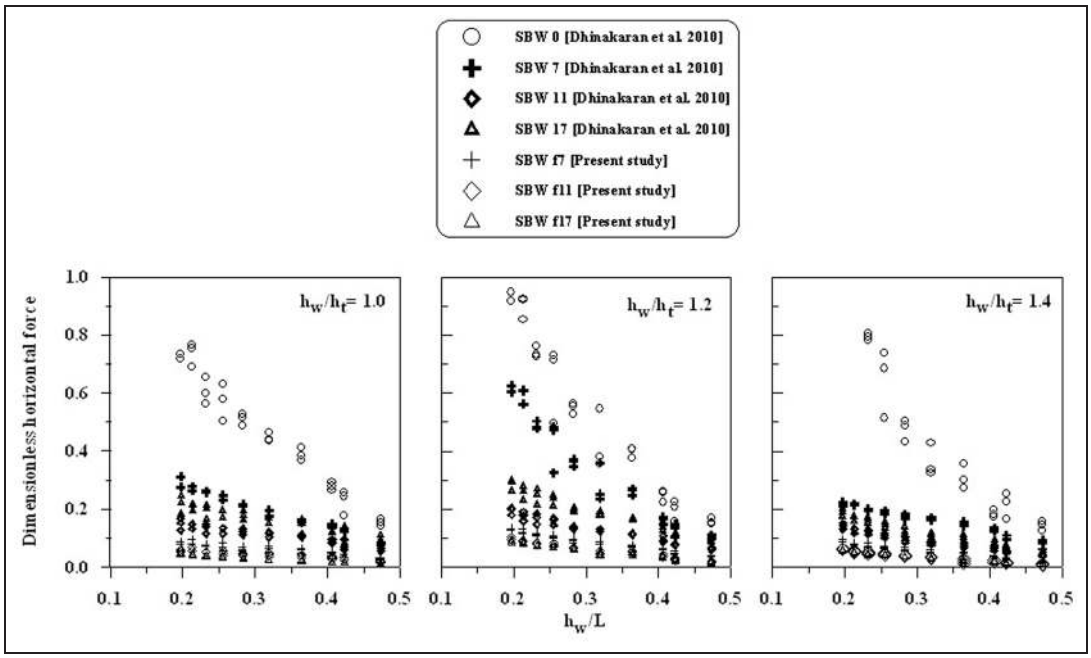

Figure 16. Effect of the water depth and perforations on the dimensionless horizontal force due to regular waves.

perforations due to the action of regular and random waves for three different water depths under submerged conditions. The above-stated characteristics for the fully perforated SBW models were compared with the results of Dhinakaran et al.[29] and salient conclusions arrived at in the study are as follows.

1. The increase in the percentage of perforations from 7% to 17% decreases the reflection coefficient and the transmission coefficient in the case of fully perforated SBWs and it was found that the maximum energy was transferred for SBWf17.
2. Of the three different h_w/h_t ratios tested, from a hydrodynamic performance viewpoint, $h_w/h_t = 1.2$ showed a better performance and experienced maximum horizontal and vertical forces; for this reason, main structures such as a vertical breakwater will be subjected to least force.
3. The magnitude of the dimensionless vertical force was equal to almost four times the horizontal force for the all the fully perforated SBW models tested and it is noteworthy that a vertical force which acts on the semicircular caisson adds stability to the breakwater.

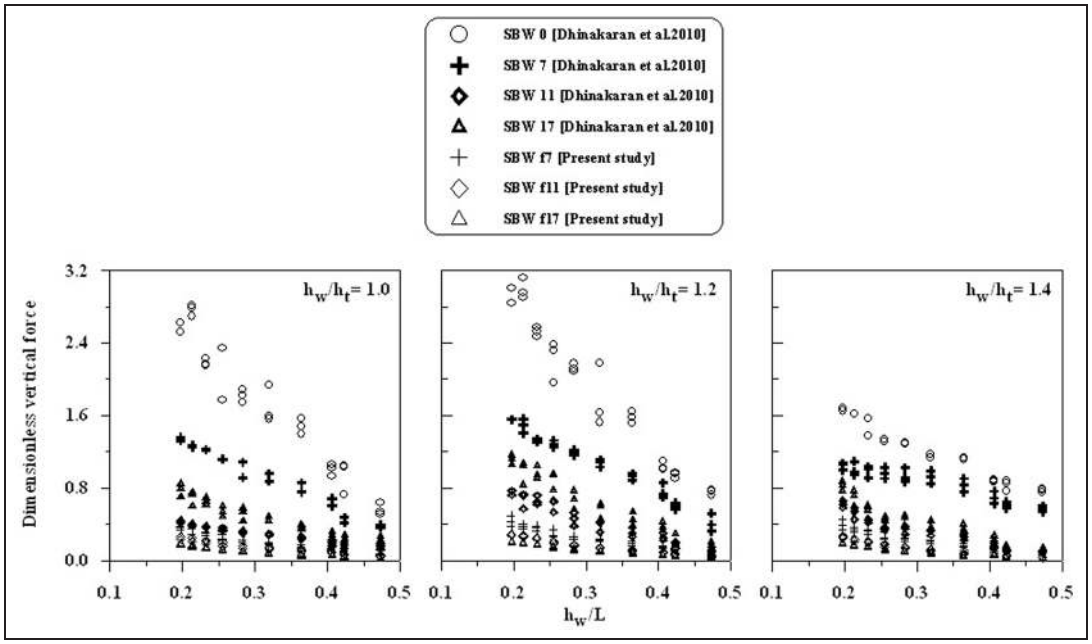

Figure 17. Effect of the water depth and perforations on the dimensionless vertical force due to regular waves.

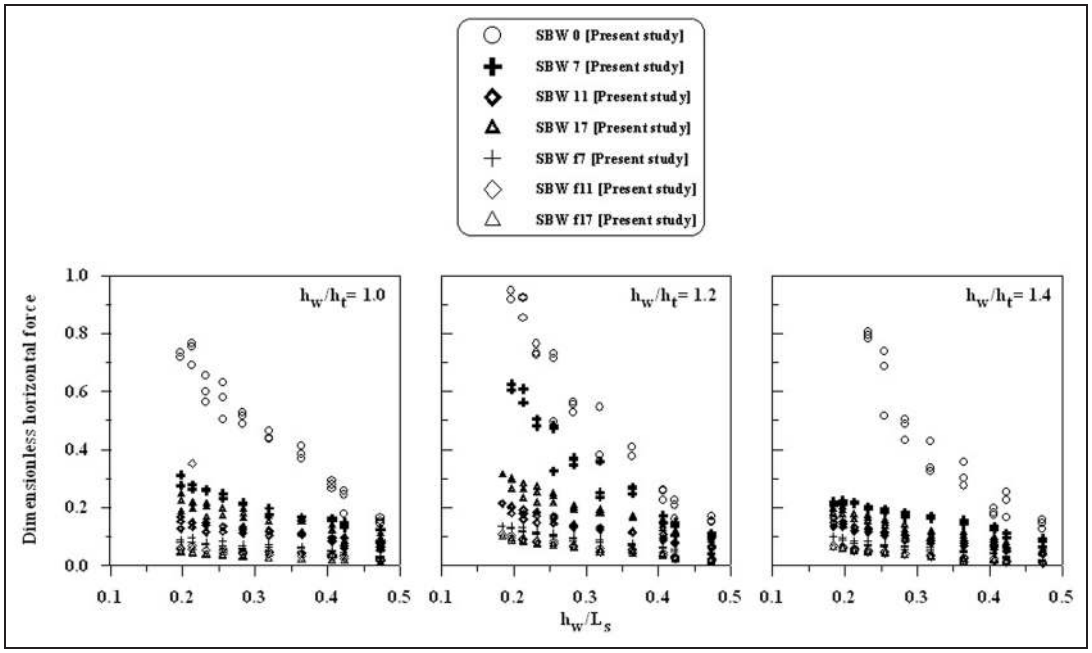

Figure 18. Effect of the water depth and perforations on the dimensionless horizontal force due to random waves.

4. Similar to forces, the dimensionless pressure also decreases with increases in the relative water depth and the percentage of perforations. An increase in h_w/h_t to 1.2 increases the pressure and a further increase in h_w/h_t reduces the pressure on the model; hence $h_w/h_t = 1.4$ is not recommended.
5. From a comparison of the results obtained for the pressure when studying the effect of perforations on the water depth, it is concluded that the variation in the magnitude of the pressure due to this effect is less significant.
6. The optimum percentage of perforation arrived in the case of fully perforated SBWs is 11% from the experiments conducted in terms of the hydrodynamic performance. The total height of the model recommended is about 1.2 times the water depth.

Funding

This work was supported by the Deutsche Gesellschaft fuer Technische Zusammenarbeit (GTZ) (grant number

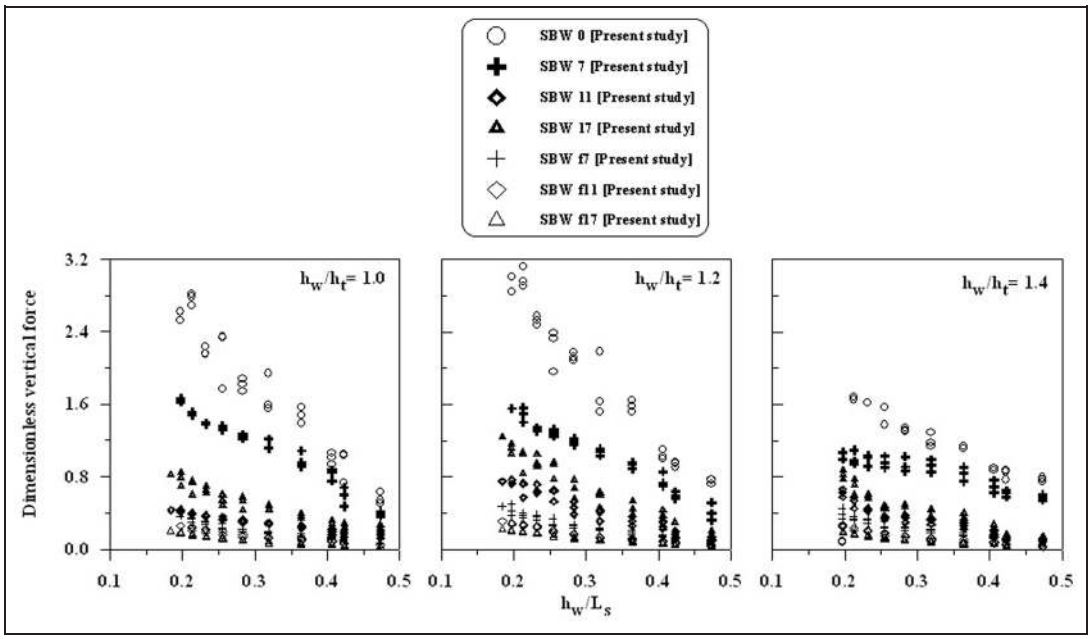

Figure 19. Effect of the water depth and perforations on the dimensionless vertical force due to random waves.

50876088). The first author was supported by SASTRA University management (grant number) during his doctoral programme at IIT Madras.

Acknowledgements

The results reported in this paper are part of a joint research project between the two collaborating institutes Indian Institute of Technology Madras, India, and University of Leipzig, Germany. The first author gratefully acknowledges SASTRA University management for the sponsorship provided during his doctoral programme at Indian Institute of Technology Madras. The authors wish to record their thanks to the Department of Ocean Engineering, Indian Institute of Technology Madras, for providing all the test facilities for the experimental studies and also to GTZ, Germany.

References

1. Ranasinghe R and Turner I. Shoreline response to submerged structures: a review. *Coastal Engng* 2006; 53: 65–79.
2. Ting CL, Lin MC and Cheng CY. Porosity effects on non-breaking surface waves over permeable submerged breakwaters. *Coastal Engng* 2004; 50: 213–224.
3. Losada IJ, Losada MA and Martin FL. Experimental study of wave-induced flow in a porous structure. *Coastal Engng* 1995; 26: 77–98.
4. Losada IJ, Silva R and Losada MA. 3-D non-breaking regular wave interaction with submerged breakwaters. *Coastal Engng* 1996; 28: 229–248.
5. Losada IJ, Silva R and Losada MA. Interaction of non-breaking directional random waves with submerged breakwaters. *Coastal Engng* 1996; 28: 249–266.
6. Losada IJ, Patterson MD and Losada MA. Harmonic generation past a submerged porous step. *Coastal Engng* 1997; 31: 281–304.
7. Mase H, Takeba K and Oki SI. Wave equation over permeable rippled bed and analysis of Bragg scattering of surface gravity waves. *J Hydraul Res* 1995; 27: 587–601.
8. Ting CL, Lin MC and Kuo CL. Bragg scattering of surface waves over permeable rippled beds with current. *Phys Fluids A* 2000; 12: 1382–1388.
9. Zhu S. Water waves within a porous medium on an undulating bed. *Coastal Engng* 2001; 42: 87–101.
10. Rojanakamthorn S, Isobe M and Watanabe A. A mathematical model of wave transformation over a submerged breakwater. *Coastal Engng Japan* 1989; 31: 209–234.
11. Dalrymple RA, Losada MA and Martin PA. Reflection and transmission from porous structures under oblique wave attack. *J Fluid Mech* 1991; 224: 625–644.
12. Hur DS and Mizutani N. Numerical estimation of wave forces acting on a three-dimensional body on submerged breakwater. *Coastal Engng* 2003; 47: 329–345.
13. Tsai CP, Chen HB and Lee FC. Wave transformation over submerged permeable breakwater on porous bottom. *Ocean Engng* 2006; 33: 1623–1643.
14. D'Angremond K, van der Meer JW and De Jong RJ. Wave transmission at low-crested structures. In: *25th international conference on coastal engineering*, Orlando, Florida, USA, 2–6 September 1996, pp. 2418–2427. Reston, Virginia: American Society of Civil Engineers.
15. Loveless J, Debski D and Macleod AB. Sea level set-up behind detached breakwaters. In: *26th international conference on coastal engineering*, Copenhagen, Denmark, 22–26 June 1998, pp. 1665–1678. Reston, Virginia: American Society of Civil Engineers.
16. Seabrook SR and Hall KR. Wave transmission at submerged rubble mound breakwaters. In: *26th international conference on coastal engineering*, Copenhagen, Denmark, 22–26 June 1998, pp. 2000–2013. Reston, Virginia: American Society of Civil Engineers.
17. Mase H, Miyahira A and Hedges TS. Random wave run-up on seawalls near shorelines with and without artificial reefs. *Coastal Engng J* 2004; 46(3): 247–268.

18. Garcia N, Lara JL and Losada IJ. 2-D numerical analysis of near-field flow at low-crested permeable breakwaters. *Coastal Engng* 2004; 51: 991–1020.
19. Cokgor S and Sedat Kapdasli M. Performance of submerged breakwaters as environmental friendly coastal structures. In: Zimmermann C (ed.) *Environmentally friendly coastal protection*. Berlin: Springer, 2005, pp. 211–218.
20. Jaafar Sidek F and Abdul Wahab MA-J. The effects of porosity of submerged breakwater structures on non-breaking wave transformations. *Malaysian J Civil Engng* 2007; 19(1): 17–25.
21. Jeng DS, Schacht C and Lemckert C. Experimental study on ocean waves propagating over a submerged breakwater in front of a vertical seawall. *Ocean Engng* 2005; 32: 2231–2240.
22. Chen HB, Tsai CP and Chiu JR. Wave reflection from vertical breakwater with porous structure. *Ocean Engng* 2006; 33: 1705–1717.
23. Aburatani S, Koizuka T, Sasayama H, Tanimato K and Namerikawa N. Field test on a semi-circular caisson breakwater. *Coastal Engng Japan* 1996; 39(1): 59–78.
24. Xie SL. Wave forces on submerged semi circular breakwaters and similar structures. *China Ocean Engng J* 1999; 13(1): 63–72.
25. Xie SL. Design of semi circular breakwaters and estuary jetties. In: *29th IAHR congress* Beijing, People's Republic of China, 16–21 September 2001, pp. 90–95. Beijing: Tsinghua University Press.
26. Dhinakaran G, Sundar V, Sundaravadivelu R and Graw KU. Dynamic pressures and forces exerted on impermeable and seaside perforated semicircular breakwaters due to regular waves. *Ocean Engng* 2002; 29(15): 1981–2004.
27. Dhinakaran G, Sundar V, Sundaravadivelu R and Graw KU. Hydrodynamic characteristics of seaside perforated semicircular breakwaters due to random waves. *J Waterway, Port, Coastal Ocean Engng* 2008; 134(4): 237–251.
28. Dhinakaran G, Sundar V, Sundaravadivelu R and Graw KU. Effect of perforations and rubble mound height on wave transformation characteristics of surface piercing semicircular breakwaters. *Ocean Engng* 2009; 36(15–16): 1182–1198.
29. Dhinakaran G, Sundar V, Sundaravadivelu R and Graw KU. Regular wave measurements on submerged semicircular breakwater. *Trans ASME, J Offshore Mech Arctic Engng* 2010; 132(3): 034501-1–034501-6.

Appendix

Notation

a	radius of the semicircular breakwater
h_r	height of the rubble mound (m)
h_s	height of the semicircular caisson (m)
h_t	total height of the breakwater (m)
h_w	depth of water (m)
h_w/L	relative water depth
H	wave height for regular waves
H_s	significant wave height for random waves
K_l	loss coefficient
K_r	reflection coefficient
K_t	transmission coefficient
l	length of the breakwater
L	length of the regular wave (m)
L_s	length of the random wave (m)
X	force component in the direction of wave propagation
z/h_w	pressure port location
Z_1, Z_2, Z_3	force components in the vertical direction
γ	density of water

Abbreviations

SBW	semicircular breakwater
SBWf7	fully perforated semicircular breakwater with 7% perforations
SBWf11	fully perforated semicircular breakwater with 11% perforations
SBWf17	fully perforated semicircular breakwater with 17% perforations
SBW0	impermeable semicircular breakwater or semicircular breakwater with no perforations
SBW7	semicircular breakwater with 7% perforations on its sea side
SBW11	semicircular breakwater with 11% perforations on its sea side
SBW17	semicircular breakwater with 17% perforations on its sea side